The response of Dual-leucine zipper kinase (DLK) to nocodazole: evidence for a homeostatic cytoskeletal repair mechanism

Laura DeVault[1], Chase Mateusiak[2,3], John Palucki[1], Michael Brent[2,3], Jeffrey Milbrandt[2,4], Aaron DiAntonio[1,4,5,*]

1. **Department of Developmental Biology, Washington University School of Medicine, St. Louis, Missouri 63110, USA.**
2. **Department of Genetics, Washington University School of Medicine, St. Louis, Missouri 63110, USA.**
3. **Department of Computer Science & Engineering, Washington University, St. Louis, MO, 63108**
4. **Needleman Center for Neurometabolism and Axonal Therapeutics, Washington University School of Medicine, St. Louis, Missouri 63110, USA.**
5. **Lead Contact**

*** Corresponding author: diantonio@wustl.edu**

Abstract

Genetic and pharmacological perturbation of the cytoskeleton enhances the regenerative potential of neurons. This response requires Dual-leucine Zipper Kinase (DLK), a neuronal stress sensor that is a central regulator of axon regeneration and degeneration. The damage and repair aspects of this response are reminiscent of other cellular homeostatic systems, suggesting that a cytoskeletal homeostatic response exists. In this study, we propose a framework for understanding DLK mediated neuronal cytoskeletal homeostasis. We demonstrate that a) low dose nocodazole treatment activates DLK signaling and b) DLK signaling mitigates the microtubule damage caused by the cytoskeletal perturbation. We also perform RNA-seq to discover a DLK-dependent transcriptional signature. This signature includes genes likely to attenuate DLK signaling while simultaneously inducing actin regulating genes and promoting actin-based morphological changes to the axon. These results are consistent with the model that cytoskeletal disruption in the neuron induces a DLK-dependent homeostatic mechanism, which we term the Cytoskeletal Stress Response (CSR) pathway.

Introduction

Injury to peripheral axons leads to cytoskeletal disassembly, axon transport disruption, and axon retraction. However, injury also stimulates repair processes that result in axon regeneration (Ertürk et al., 2007; Kerschensteiner et al., 2005). While cytoskeletal disassembly is a feature of the early stages of peripheral neuron injury, cytoskeletal reassembly is a hallmark of the later stages (Ghosh-Roy et al., 2012; Lu et al., 2015). One central participant in the axon regeneration program is Dual-Leucine Zipper Kinase (DLK), which is activated by injury and other neuronal stressors (Hammarlund et al., 2009; Miller et al., 2009; Shin et al., 2012; Xiong et al., 2010). It has been hypothesized that DLK regulates an axonal stress response (Asghari Adib et al., 2018). While the axon is an important locus of DLK action, this response is may be neuron-wide since whole neuron treatment with cytoskeletal disrupting drugs exerts greater DLK-dependent effects than axonal compartmentalized treatments (Valakh et al., 2015) and DLK signaling dramatically impacts dendritic morphology (Wang et al., 2013).

DLK-dependent signaling cascades occur after physical injury of the axon, deprivation of nerve growth factor (NGF), and treatment with low doses of either the microtubule destabilizer nocodazole or the actin destabilizer cytochalasin D (Sengupta Ghosh et al., 2011; Valakh et al., 2015). Each of these treatments disrupts the cytoskeleton. Nocodazole and cytochalasin D directly impact the microtubule or actin cytoskeleton, while physical injury and NGF deprivation impact the cytoskeleton through microtubule fragmentation and actin loss (Unsain et al., 2018; Wang et al., 2019).

While DLK activation is transiently induced during development or injury, constitutive DLK signaling is observed upon genetic perturbation of cytoskeletal components and regulators. In *C. elegans*, loss of β-spectrin, a core component of the neuronal membrane periodic structure, increases neuronal susceptibility to mechanical strain and activates DLK signaling (Hammarlund et al., 2009). Similarly, in *Drosophila*, DLK signaling is constitutively activated by loss of Spectraplakin, a linker of the actin and microtubule cytoskeleton, Patronin, a minus-end microtubule capping protein, and Rae1, a microtubule binding protein (Chuang et al., 2014; Feng et al., 2019; Tian et al., 2011; Valakh et al., 2013). Loss of Spectraplakin, Patronin and Rae1 each increase cytoskeletal instability in the axon (Feng et al., 2019; Richardson et al., 2014; Valakh et al., 2013). These findings collectively suggest that cytoskeletal instability activates DLK signaling.

Upon activation, DLK initiates a MAP kinase signaling cascade. DLK's major direct phosphorylation target is MKK4, which in turn phosphorylates JNK (Hammarlund et al., 2009; Itoh et al., 2014). In the axon, DLK activation triggers the retrograde transport of the DLK/MKK4/JNK complex to the cell body, leading to phosphorylation of the transcription factor cJun (Huntwork-Rodriguez et al., 2013; Sengupta Ghosh et al., 2011; Shin et al., 2012; Xiong et al., 2010). Arrival of the injury signal at the nucleus results in a suite of transcriptional changes, including the induction of cJun and other regeneration-associated genes (Lindwall et al., 2004; Shin et al., 2019; Watkins et al., 2013). These transcriptional changes promote axon outgrowth, a process driven by coordinated interaction of microtubules, actin and microfilaments. These genes, including cJun, are transiently expressed. Within days, injured neurons *in vitro* return to a basal state (Frey et al., 2015).

A homeostatic response is a regulatory process in which a disruption triggers a mechanism that returns the system to the basal state. In this work, we evaluate the hypothesis that a DLK-dependent cytoskeletal homeostatic network exists. We propose the following criteria: (1) cytoskeletal perturbation must initiate a DLK signaling cascade resulting in (2) transcriptional changes which include (3) genes capable of attenuating the strength of the DLK signaling cascade and (4) genes capable of modulating the cytoskeleton, thus resulting in (5) changes in and ultimately repair of damage to the cytoskeleton. To investigate the hypothesis that such a cytoskeletal homeostatic network exists, we test the impact of low dose nocodazole treatment on cultured dorsal root ganglia (DRG) sensory neurons. Our findings demonstrate that cytoskeletal perturbation activates DLK signaling and generates a DLK-dependent transcriptional signature. This transcriptional signature includes both cytoskeletal regulators and MAP kinase signal attenuators. Moreover, inhibiting this DLK pathway exacerbates microtubule defects induced by low dose nocodazole. These results are consistent with the model that, upon cytoskeletal disruption, neurons engage a DLK-dependent homeostatic mechanism that we term the Cytoskeletal Stress Response pathway (CSR).

Results

Treatment with Low Dose Nocodazole Induces DLK-dependent Signal Transduction in Cultured Neurons

Treatment with low dose nocodazole, a cytoskeletal perturbing drug, increases axon regeneration. This response requires DLK and JNK (Valakh et al., 2015), suggesting that low dose nocodazole treatment activates DLK and downstream MAP kinases (Cavalli et al., 2005; Fan et al., 1996). To test this facet of our hypothesis, we evaluated the interaction of low dose nocodazole and DLK inhibitor in cultured DRG neurons by pretreatment with DLK inhibitor (500nM) and subsequent 16 hour treatment with low dose nocodazole (200nM). This dose of nocodazole mildly perturbs the cytoskeleton, diminishing microtubule polymerization, but not microtubule density, after 4 hours (Jaworski et al., 2009). To determine if the DLK signaling cascade is activated in these conditions, we examined the phosphorylation of MKK4, a direct target of DLK (Yang et al., 2015). After 4 hours of treatment, there is an increase in the ratio of phosphorylated MKK4 to MKK4, indicating the activation of the MAP3K signaling cascade (Fig 1 A,B). Previous studies demonstrate that activation of a DLK retrograde signaling cascade induces transcription and phosphorylation of cJun, a transcription factor associated with regeneration. Indeed, treatment with low dose nocodazole was previously shown to induce cJun phosphorylation in DRGs in a DLK dependent manner (Valakh et al., 2015). We verified that low dose nocodazole induced cJun protein expression in a DLK-dependent manner (Fig 1 C,D). These results confirm that treatment with low dose nocodazole activates DLK signaling resulting in increased expression of the transcription factor cJun, thus demonstrating criteria (1) cytoskeletal perturbation activates the DLK signaling cascade.

We examined neuronal cultures to determine the effect of nocodazole on axon morphology. After 16 hours of nocodazole treatment, we consistently observed prominent growth cones consisting of broad lamellipodial structures as well as numerous short branches extending from the primary axon (Fig 1E). These nocodazole-dependent effects did not occur with DLKi pretreatment. In addition, pretreatment with DLKi inhibitor independently changed axon morphology. Within minutes of DLK inhibitor application, growth cones disappeared. By 16 hours after pretreatment with DLK inhibitor, swellings and protrusions appeared along the most distal portions of the axon. In subsequent experiments, we characterized and quantified changes to axonal morphology.

Since nocodazole inhibits microtubule polymerization, we examined the impact on microtubule integrity. As predicted from prior studies which use low dose of nocodazole (Jaworski et al., 2009), microtubule integrity was maintained in control and nocodazole treated neurons. This result is shown by staining for β-tubulin (Fig 1F,G). To determine the DLK dependence of microtubule maintenance, we evaluated the effect of DLK inhibitor on neurons treated with DMSO (control) and nocodazole. We observed no defects in DLK inhibitor treated neurons. However, DLK inhibition in nocodazole-treated neurons causes defects to the microtubule cytoskeleton, including gapping within the microtubules leading to a bead-on-a-string appearance along the axon. Quantification of microtubule continuity demonstrates a significant defect upon DLK inhibition in nocodazole-treated neurons (Fig 1F,G). This suggests that DLK signaling is required to mitigate the long-term impact of nocodazole treatment on microtubule structure in the axon. We next investigated if transcriptional changes contribute to these alterations in axon morphology.

Transcriptional Profiling Reveals a DLK-dependent Genetic Program Activated by Low Dose Nocodazole Treatment

To gain insights into DLK-dependent transcriptional changes following cytoskeletal insult, we performed bulk RNA sequencing on cultured neurons treated for 16 hours with low dose nocodazole. We determined the transcriptional effects of nocodazole treatment, DLK inhibition and the interaction of nocodazole and DLK inhibitor. Our analysis identified DLK-dependent effects of nocodazole (Fig 2A). In a principal components analysis, we observed that treatment with nocodazole led to a DLK-dependent clustering of samples along PC1, an axis accounting for 57% of the variability in the transcriptome (Fig 2B). This suggests that cytoskeletal perturbation has a major effect on neurons' transcriptional profiles (corresponding to a major shift on PC1) that is abrogated by DLK inhibitor.

Among the DLK-dependent nocodazole-dependent differentially expressed genes, the four most upregulated genes were the transcription factors Jun, Egr1, and Atf3 and the signaling regulator, Dusp1 (Fig 2C). Indeed, increased Jun transcription is consistent with the increase in its protein expression which we observed after nocodazole treatment (Fig 1 C,D). Jun is a downstream target of the DLK/JNK pathway, which is phosphorylated and activated by JNK. Hence, the transcriptional upregulation of Jun is likely an amplification of the DLK signal, which can lead to apoptosis if the induction is sustained (Bossy-Wetzel et al., 1997). Concurrently, upregulation of

Dual Specificity Protein Phosphatase (DUSP) genes indicates the activation of pathways that attenuate the same DLK signal. This suggests a feedback mechanism which is a hallmark of a homeostatic system. DUSPs are potent negative regulators of MAP kinase activity. DUSPs main function is to dephosphorylate and inactivate MAPKs (An et al., 2021). Expression of both cytoplasmic DUSPs associated with the p38/JNK pathway (Dusp16, Dusp8, and Dusp10) and inducible nuclear DUSPs (Dusp1, Dusp4, and Dusp5) increased after nocodazole treatment in a DLK-dependent manner. Additional negative phosphorylation regulators (Timp3, Cnksr3, Trib1, Per1, Spry1, Sfrp4, Spred2, Ppp1r15a, Spred3, Sema6a, Inpp5j, Lrrk2, Casp3) are differentially expressed after nocodazole treatment in a DLK-dependent manner (Fig. 2E). Therefore, nocodazole treatment induces DLK-dependent transcriptional changes that likely regulate and attenuate DLK signaling, thereby supporting homeostatic criteria (3) that a cytoskeletal homeostatic program attenuates signaling and returns the cell to baseline.

To gain a more comprehensive understanding of the differentially expressed genes that are both DLK-dependent and nocodazole-dependent, we used Gene Ontology (GO) term based gene set enrichment analysis (GSEA) (Fig 2D-I). Many of the downregulated GO terms are associated with the function of mature neurons. These include terms associated with synapses, neurotransmitter, neuropeptides, behavior, pain, and motor function. In contrast, the upregulated terms are generally associated with stressed or immature/regenerating neurons, kinase regulation, and cytoskeleton, including terms for polarized growth, response to ER stress, kinase regulation, transcriptional regulation, and the actin-rich cell cortex and microtubule-rich centrosomes. Taken together, this suggests that nocodazole treatment activates a DLK-dependent program that regulates transcriptional activity through transcription factors and MAP kinase regulators. Activation of this program downregulates mature neuron behaviors and upregulates both stress response and growth genes. This program increases expression of genes related to polarized neuron growth, including genes regulating the cytoskeleton.

Low dose nocodazole induces DLK-dependent transcriptional and morphological changes to the actin cytoskeleton.

We noted that GO and KEGG pathway terms related to the cytoskeleton were significantly overrepresented in our data set. KEGG pathway analysis identified significant enrichment in Focal Adhesions, driven by differential expression of Jun, Itga5, Shc4, Zyx, Shc3, Tnc, Itga9, Bcl2, Pxn, Flnb, Pik3cb (Fig 3A). Focal adhesions are associated with actin-integrin structures which regulate actin dynamics. In addition, GO GSEA of differentially expressed genes revealed enrichment in the Actin Cytoskeleton and Cytoskeleton Organization (Fig 3B). Differentially expressed genes with at least a four-fold change included 12 genes associated with Cytoskeletal Organization, of which 9 belong to Actin Cytoskeleton Organization including: Sipa1l1, Zyx, Rnd3, Palld, Phldb2, Rhpn2, Ptger4, Tmod1, Bcl6 and Arc. Arc regulates actin in dendritic spine formation (Messaoudi et al., 2007). Lrguk is associated with ciliary assembly (Liu et al., 2015), while Stmn4 is a well-established microtubule regulator that sequesters free tubulin (Nakata et al., 2005). Stmn4 is notable as a highly expressed transcript consistently associated with DLK data sets (Fig 3B) (Larhammar et al., 2017; Maor-Nof et al., 2016; Tian et al., 2019). These findings suggest that nocodazole treatment induces a transcriptional program that affects the cytoskeleton primarily through actin regulation, fulfilling criteria (4) that a cytoskeletal homeostatic program upregulates expression of cytoskeletal genes. We independently verified a subset of these differentially expressed genes by quantitative PCR (qPCR) (Fig 3C).

To investigate whether morphological alterations to the actin cytoskeleton occurred in concert with the transcriptional changes, we examined the axon and growth cone. Along the axon, short protrusions emerge after nocodazole treatment (Fig. 4A). These protrusions resemble actin-rich filopodia and immunostaining with the f-actin marker phalloidin confirmed the presence of actin so we identify these protrusions as filopodia (Mattila and Lappalainen, 2008). The number of filopodia significantly increased after 16 hours of nocodazole treatment (Fig. 4C). In addition to regulating filopodia, increased actin dynamics at the growth cone also mediates axon extension. Therefore, we tested the influence of nocodazole on growth cone morphology, and observed a significant increase in the size of the growth cone following nocodazole treatment (Fig 4. B,D). Both the increased number of filopodia and larger size of growth cones is DLK dependent (Fig 4A-D). These findings demonstrate that cytoskeletal perturbation triggers DLK-dependent changes in actin morphology, addressing criteria (5) that cytoskeletal repair occurs in a DLK-dependent manner.

Taken together, these findings demonstrate that low-dose nocodazole treatment induces DLK-dependent changes to the actin cytoskeleton, with upregulation of genes associated with Actin Cytoskeleton Organization and concomitant emergence of actin-rich filopodia along the axon and an increase in size of the growth cone.

Hence, disrupting the cytoskeleton via low dose nocodazole leads to DLK-dependent transcriptional and morphological changes to the neuronal actin cytoskeleton.

DLK-dependent transcriptional changes after nocodazole treatment are similar to transcriptional changes after NGF deprivation.

To investigate the existence of a DLK-dependent transcriptional signature common to various insults that cause neuronal cytoskeletal stress, we compared the DLK-dependent effects of nocodazole to those induced by NGF deprivation. To do this, we compared our data (effect_of_dlki_noc) to the effects of NGF deprivation versus DLK inhibitor (dlki_vs_dmso_ngf_minus) in cultured DRGs (Larhammar et al., 2017).

We found a large and highly significant correlation between differentially expressed genes after nocodazole treatment and NGF deprivation in cultured sensory neurons (Fig. 5A) We identified 1098 differentially expressed genes shared between the two data sets (Fig 5B-C). Among these, thirteen genes exhibited a greater than four-fold gene expression change in the same direction in both datasets (Dusp1, Htr4, Atf3, Irf6, Dusp16, Ypel4, Arid5a, Egr1, Dact2, Gprc5c, Jun, Creb5, Sh2d3c), demonstrating that MAP kinase negative regulators (Dusp1, Dusp16), transcription factors (Atf3, Egr1, Jun, Creb5, Irf6) transcriptional regulators (Arid5a, Dact2), scaffold proteins (Sh2d3c), membrane integrity regulators (Ypel4) and G-coupled proteins (Gprc5c) are abundantly upregulated by DLK signaling in both paradigms. Only one gene, Htr4, a serotonin receptor, has at least a four-fold downregulation after both NGF deprivation and nocodazole treatment, consistent with a downregulation of more mature neuronal functions.

To test the hypothesis that DLK-dependent signaling results in consistent transcriptional changes to actin regulators between the low dose nocodazole and NGF deprivation datasets, we investigated the GO term Actin Cytoskeleton Organization (Fig 5D-E). Indeed, there is a significant enrichment of this term in both datasets (Low Dose Noc $p=1.626\times10^{-8}$ and NGF Deprivation $p=8.656\times10^{-11}$). In both datasets, Zyx, which coordinates actin dynamics at focal adhesions and stress fibers, is significantly upregulated. This perhaps accounts for the morphological changes that we observe in nocodazole treated neurons. We also observe a greater than two-fold downregulation of the following: Fmnl1, a formin-like protein, Tacr1, a transmembrane receptor and Rhpn2, a Rho-GTPase binding protein which may limit stress fiber formation (Peck et al., 2002). These results suggest that diverse mechanisms of DLK activation result in differential expression of actin cytoskeleton regulators, consistent with the hypothesis that neurons engage a DLK-dependent cytoskeletal homeostatic network in response to perturbation.

Discussion

In this work, we explore the hypothesis that DLK regulates a homeostatic network that responds to cytoskeletal damage and facilitates cytoskeletal repair, a process we term the Cytoskeletal Stress Response (CSR) pathway. To determine if this pathway exists, we evaluate the following five criteria in this paper: (1) cytoskeletal perturbation must initiate a DLK signaling cascade resulting in (2) transcriptional changes which include (3) genes capable of attenuating the strength of the DLK signaling cascade and (4) genes capable of modulating the cytoskeleton, thus resulting in (5) changes in and ultimately repair of damage to the cytoskeleton. Here, we discuss the current evidence for a CSR-pathway and identify existing gaps in evidence required to establish the CSR as a homeostatic response.

DLK plays a critical role in sensing and responding to cytoskeletal damage

We demonstrate that cytoskeletal damage activates a DLK signaling cascade. This result is consistent with published work identifying pharmacologic and genetic perturbations of the cytoskeleton that activate DLK dependent stress signaling in neurons (Chen et al., 2015; Chuang et al., 2014; Feng et al., 2019; Ghosh-Roy et al., 2012; Hammarlund et al., 2009; Valakh et al., 2015, 2013). While these findings support the idea that cytoskeletal stress activates DLK, we lack a mechanistic understanding of how cytoskeletal disruption activates DLK. In fact, seemingly disparate genetic perturbations of the cytoskeleton activate DLK signaling, including mutations in Spectraplakin, an actin microtubule linking protein, Camsap, a minus end microtubule capping protein, and Beta-spectrin, a scaffolding protein essential for membrane integrity (Zhang et al., 2017). The exception to this set of unknown intermediaries between perturbation and DLK activation is Rae1, a WD40 microtubule interactor, which affects DLK via regulating the levels of the E3 ubiquitin-protein ligase, Highwire (Tian et al., 2011), which in turn ubiquitinates and promotes the degradation of DLK (Collins et al., 2006; Nakata

et al., 2005). In sum, the mechanisms linking cytoskeletal perturbation to DLK activation are almost entirely unknown.

Unlike the intermediaries between cytoskeletal perturbation and DLK activation, the DLK signaling cascade itself is well established. DLK phosphorylates a MAP2K, either MKK4 or MKK7, which in turn phosphorylates a MAPK, either JNK or p38 (Itoh et al., 2014; Watkins et al., 2013). Phosphorylation and palmitoylation of DLK and JNK drives association with retrograde trafficked vesicles (Holland et al., 2016; Tortosa et al., 2022). The retrograde trafficking of these signaling molecules results in increased transcription and phosphorylation of the transcription factor, Jun, which is critical for DLK-dependent increases in neuron regeneration (Lindwall et al., 2004; Shin et al., 2012). We find that the transcription factors, Jun, Egr1, and Atf3 exhibit the greatest DLK-dependent changes after cytoskeletal disruption. While Jun can promote axon regeneration, it is also a key driver of apoptosis (Dragunow et al., 1993), and DLK-dependent retrograde signaling promotes retinal ganglion cell death after optic nerve injury (Watkins et al., 2013; Welsbie et al., 2013). Interestingly, the DLK-dependent expression of DUSPs, which negatively regulate DLK/JNK signaling, and so likely mitigate the strength of the Jun signal, may play a key role in ensuring that DLK activation results in axon regeneration rather than apoptosis in DRG neurons. Furthermore, DUSPs may act upon the cytoskeleton. Of particular interest, Dusp1 regulates axonal branching through JNK-dependent cytoskeletal remodeling (Jeanneteau et al., 2010). Interestingly, Atf3 promotes axon regeneration in retinal ganglion cell models (Jacobi et al., 2022; Renthal et al., 2020), but can also regulate degenerative pathways (Tian et al., 2022). Egr1, an immediate early gene associated with neuronal activity, is also linked to regeneration in spinal cord injury (Milbrandt, 1987; Yin et al., 2023). It will be important to understand the role of Atf3, Egr1 and the DUSP genes in the DLK-dependent axon injury program.

Evidence for homeostatic repair comes from observations of axon growth and maintenance of cytoskeletal integrity. We demonstrate that DLK is required for the integrity of the axonal microtubule cytoskeleton after perturbation with nocodazole. While we did not prove that this effect is due to the expression of DLK-dependent genes, this finding is consistent with the model that a DLK-dependent mechanism repairs damage to the cytoskeleton. Increased axon growth is a well-documented consequence of activating DLK signaling cascades (Hammarlund et al., 2009; Shin et al., 2012; Valakh et al., 2015; Watkins et al., 2013; Xiong et al., 2010). Both phenomena may be mechanistically linked to the genetic changes we observe. We demonstrate that nocodazole treatment induces DLK-dependent expression of actin regulatory genes and results in broad changes to the actin cytoskeleton, including increased filopodia number along the axon and enlarged growth cones. As nocodazole predominantly acts on the microtubule cytoskeleton, the extensive engagement of actin regulatory mechanisms is unexpected. There are two potential explanations for this incongruity. First, our response may reflect coordination between the actin and microtubule cytoskeleton. Initial reorganization of the actin cortical cytoskeleton precedes coordinated polymerization between the actin and microtubule cytoskeleton into primary axon branches (Dent and Kalil, 2001; Gallo and Letourneau, 1999). As such, our results may reflect an early stage of outgrowth, preceding microtubule extension into the growth cone. Second, the predominance of actin-related transcripts may reflect a unique role for actin regulation in repairing neuronal structures, as suggested by work which demonstrates that actin turnover drives regeneration (Tedeschi et al., 2019). Actin structures may also influence microtubule integrity, as microtubule lattice repair occurs more frequently in stress fiber adjacent regions (Gazzola et al., 2023). Although the transcriptional response predominantly consists of actin regulators, transcription of a microtubule regulatory gene, Stmn4, is strongly increased after nocodazole treatment. Future work will explore the importance of Stmn4 for microtubule integrity and extension into the growth cone.

While not demonstrated in this paper, we predict that the CSR repairs the axonal cytoskeleton at the subcellular scale. In particular, it would be interesting if DLK activation promoted repair of the membrane periodic structure of the axon, an interconnected sub membrane structure of repeating β-spectrin and actin rings that provides strength and flexibility to axons (Costa et al., 2020; Leterrier, 2021). Of note, disassembly of the membrane periodic structure (MPS) likely drives DLK activation (Wang et al., 2019). Both loss of β-spectrin and NGF deprivation disrupt the MPS and activate DLK signaling (Hammarlund et al., 2009; Unsain et al., 2018; Wang et al., 2019). Moreover, DLK activation is sensitive to the disassembly of the actin MPS after NGF deprivation. This is demonstrated by pretreatment with jasplakinolide, which stabilizes the MPS and blocks the DLK signaling cascade (Wang et al., 2019). Finally, cytoskeletal targeting drugs, including latrunculin A disrupt the MPS and activate DLK signaling (Karney-Grobe et al., 2018; Wang et al., 2019; Zhong et al., 2014). Less is known about

the consequences of activating DLK signaling for the MPS and additional studies will be required to understand if activating the CSR facilitates MPS repair and to demonstrate convincingly that cytoskeletal damage engages a DLK-dependent homeostatic network.

The CSR resembles other homeostatic networks

The CSR mirrors other homeostatic network responses, such as the UPR or heat shock response, in three ways. First, in the proposed CSR, cellular stress initiates, through DLK, a kinase signaling cascade. This is reminiscent of the way IRE acts as a kinase sensor initiating the UPR. Second, homeostatic networks are associated with transcriptional programs driven by transcription factors. After UPR activation, expression of transcription factors, Atf4, Atf6 and XBP1 drive expression of homeostatic effector genes related to protein quality control, lipid synthesis, ER-associated degradation, apoptosis and autophagy. There is strong evidence from this study and others that activated DLK signaling induces transcription through Jun, Egr1 and Atf3. We speculate that these transcription factors control expression of actin regulatory genes, negative JNK signaling regulators and the dampening of genes related to mature neuron function. Future work will delineate the relationship between these transcription factors and their targets in this pathway. Finally, like other homeostatic pathways, activation of the CSR mediates repair or cell death in a context dependent manner. In the CSR, this is particularly evident when comparing the response of retinal ganglion cells in the CNS to dorsal root ganglion cells in the PNS. While DLK activation of DRGs leads to regeneration, DLK activation in RGCs leads to apoptosis (Sengupta Ghosh et al., 2011; Shin et al., 2012; Watkins et al., 2013; Welsbie et al., 2013).

In summary, we propose that DLK acts as a sensor for the Cytoskeletal Stress Response, enabling neurons to sense and repair damage to the cytoskeleton. This model of a DLK-dependent cytoskeletal homeostatic repair mechanism is consistent with over twenty years of data placing DLK at the center of neuronal degeneration and regeneration programs. Here, we contextualize this argument in light of previous research, demonstrate that DLK signaling is required to maintain microtubule structure following disruption of microtubule polymerization, provide transcriptional analysis of DLK dependent gene expression after cytoskeletal perturbation and present evidence of actin cytoskeletal modulation. If validated, this model adds the cytoskeleton to the array of cell biological structures and processes maintained via homeostatic regulatory networks.

Acknowledgements

We thank EJ Brace and Joseph Bloom for critical reading of the manuscript, Margaret Hayne for technical help and members of the DiAntonio and Milbrandt labs for discussion. This work was supported by National Institutes of Health grants (F32NS117784 to LD, R01NS087632 to A.D. and J.M. and R37NS065053 to A.D.)

Author Contributions

LD and AD conceptualized this study and wrote this manuscript. LD and JP performed RNA sequencing experiments. CM and MB analyzed RNA sequencing data and consulted on two-factor analysis. LD performed microscopy and qPCR experiments and analysis. JM and AD supervised experiments.

Figure Legend

Figure 1. Treatment with low dose nocodazole activates DLK dependent signaling, resulting in transcriptional changes. A) Immunoblot for phospho-MKK4, MKK4 and HSP90. Cultured DRGs were pretreated with DMSO or 500nM DLKi (GNE-3511) and subsequently treated with 200nM nocodazole or DMSO. Samples were collected at 4 and 16 Hours. B) Quantification of immunoblot. A two-way ANOVA revealed there was a statistically significant interaction between the effect of DLKi and low dose nocodazole treatment (Df=16, F = 9.329, p = 0.00757). C) Immunoblot for phospho-Jun, cJun and HSP90. D) Quantification of immunoblot. A two-way ANOVA revealed there was a statistically significant interaction between the effect of DLKi and low dose nocodazole treatment (Df= 14, F = 17.04, p = 0.001024). E) Representative images of cultured neuron axons after 16 hours of treatment. Lamellipodia structures are noted with an arrow; short branching structures are noted with a triple arrow and axonal swellings are noted with diamonds. F) Axons stained for Tuj1 after 16 hours of treatment. G) Normalized microtubule fragmentation after 16 hours of treatment. A two-way ANOVA revealed a statistically significant interaction between the effect of DLKi and low dose nocodazole treatment (Df=153, F=24.16, p =2.26 x 10-6).

Figure 2. DLK inhibition on low dose nocodazole treatment impacts gene expression.A) Experimental design for RNA sequencing with two factors, pretreatment (DMSO, DLKi) and treatment (DMSO, Noc). B) Principal Component Analysis (PCA) of RNA sequencing experience for four conditions (DMSO, DMSO; DMSO, Noc; DLKi, DMSO; DLKi, Noc) with four replicates. C) Differential gene expression in cultured DRGs of DLKi in low dose nocodazole. Log2FoldChange was determined in a two factor with interaction design in DESEQ2. Log2FoldChange was plotted with regard to base mean gene expression. Genes with the greatest log2FoldChange (n=500) were selected for further analysis using WebGestalt for Gene Set Enrichment. D) Biological Process enrichment in response to ER stress (value) and negative regulation of phosphorylation (value). Nocodazole treatment increases gene expression related to Stress Response and Signaling Regulation (ER stress (GO:0034976, NES= -1.9892, p= 0.00147, FDR= 0.09715) and Negative Regulation of Phosphorylation (GO:0042326, NES= -1.9969, p= 0.0037406, FDR =0.12066)). Conversely, nocodazole treatment decreases expression of biological processes specific to mature neuronal behaviors including Pain Perception, Behavior Regulation and Feeding Behavior (Sensory Perception of Pain (GO:0019233, NES = 2.3965, p= <2.2e-16, FDR = 0.008895), Regulation of Behavior (GO:0050795, NES= 2.29, p= <2.2e-16, FDR= 0.01129), Neurotransmitter Transport (GO:0006836, NES= 2.3623, p= <2.2e-16, FDR= 0.00975) , G-protein Coupled Receptor Signaling (GO:0007187, NES= 2.6953, p = <2.2e-16, FDR= <2.2e-16) and Feeding Behavior (GO:0007631, NES= 2.772, p<2.2e-16, FDR<2.2e-16)). E) Cell compartment enrichment in cell cortex (GO:0005938, FDR 0.28243, p= 0.0057389), neuron projection terminus (GO:0044306, FDR 0.46809, p = 0.0063898) F) Molecular function enrichment in DNA-binding Transcription Activator Activity increased after nocodazole treatment in a DLK-dependent manner (NES: -2.0360, FDR: 0.043388, GO:0001228, p = 0.0027933). Conversely, Peptide Receptor, Neurotransmitter, and G-protein Coupled Receptor Activity (peptide receptor activity (NES: 2.5456, FDR: 0.00084809, GO:0001653, p < 2.2e-16), and G protein-Coupled Receptor Binding (NES: 2.0976, FDR: 0.024595, GO:0001664, p = 0.0056338) had positive enrichment scores.

Figure 3. Treatment with low dose nocodazole increases expression of cytoskeleton organization genes. A) KEGG diagram for focal adhesion NES= -2.4 (mmu04510**,** FDR = 0.0026919, p=<2.2e-16). Genes with a log2FoldChange > -0.5 are noted in red. B) Differential gene expression of DLK inhibitor in low dose nocodazole in cultured DRGs, actin cytoskeleton organization (GO:0030036, padj= 1.979×10^{-7}) noted in red, and cytoskeleton organization (GO:0007010, padj =5.452×10^{-5}) noted in blue. Cytoskeletal organization genes with a log2FoldChange greater than 2 noted. C) Differential expression of select genes (Stmn4, Zyx, Itga9) was confirmed by qPCR. Expression was normalized to Reference Genes (Ubc, Rpl27). There was a statistically significant interaction between low dose nocodazole treatment and DLK inhibitor on gene expression for Stmn4 (F=19.45, p=0.000851), Zyx (F= 4.580, p=0.05190) and itga9 (F= 9.053, p= 0.0101).

Figure 4. Low dose nocodazole increased filopodia along the axon in a DLK-dependent manner. A) Cultured DRG neurons axons expressing GFP were stained for phalloidin after 16 hours of treatment with either low dose nocodazole or DMSO (control). Neurons were pretreated with either DLKi or DMSO. B) Differences in growth cone morphology were observed at 16 hours after treatment C) We further analyzed the number of filopodia along branches and found a significant increase in short branches (less than 10 µm) in neurons treated with DMSO+Noc (27.5 +/-10.1) compared to DMSO+DMSO treated neurons (4.9 +/- 2.1), DLKi+DMSO (1.4 +/- 1.35)

DLKi+Noc (3.2 +/- 2.0). A Two-way ANOVA confirmed that the presence of actin rich branches in low dose nocodazole treated neurons was DLK dependent (Df= 35, F = 15.35, p=0.0004). D) Normalized Growth Cone area was significantly increased after low dose nocodazole treatment. A two-way ANOVA demonstrated increased growth cone area in Noc (26.5% +/- 8.6%) compared to DMSO treated neurons (14.8% +/- 5.4%), DLKi (5.7% +/- 1.5%) DLKiNoc (5.6% +/- 1.5%). (Df= 76, F=8.0, p = 0.00596).

Figure 5. Conservation of DLK-dependent injury gene expression after low dose nocodazole treatment, NGF deprivation and sciatic nerve crush. Linear models were used to analyze the similarities between the different treatments. Correlation between log2FoldChange of differential gene expression of DRGs with respect to the effect of DLKi in low dose nocodazole and (A) log2FoldChange of DLKi vs NGF deprivation (correlation p-value < 1.2 e-12). (B,C) Transcriptional comparison of differential expression in Low Dose Nocodazole and NGF deprivation paradigms, genes differentially expressed in both data sets marked in blue. Volcano plot of -log10(p-adjusted) v log2Fold Change for (C) Low Dose Nocodazole and (D) NGF Deprivation. Genes differentially expressed in both data sets with greater than 2 log2FoldChange are noted. (D,E) Actin Filament based processes (GO:0030029) are enriched in differentially expressed genes sets for Low Dose Noc ($p=1.626\times10^{-8}$) and NGF Deprivation ($p=8.656\times10^{-11}$). Genes belonging to GO: Actin filament-based process (GO:0030029) displayed in red. Actin Cytoskeleton Organization genes (GO:0030029) with absolute log2Fold Change > 1 present in both datasets are noted (Zyx, Gab1, Fmnl1, Tacr1, Rhpn2).

Methods

Primary embryonic DRG culture

Primary DRGs were cultured from E13.5 CD1 mouse embryos (Charles River Laboratories). DRGs were dissected in DMEM. Once isolated, DRGs were incubated in 0.5% trypsin, 0.05% EDTA for 13 minutes. Neurons were resuspended in growth media (Neurobasal (Gibco), 2% B27 (Invtrogen), 50 ng/ml nerve growth factor (Harlan Laboratories), 1 µM 5-fluoro-2'-deoxyuridine (Millipore Sigma), 1 µM uridine (Millipore Sigma), and penicillin/ streptomycin (Thermo Fisher Scientific)) and spotted onto PDL poly-D-lysine, laminin coated plates. After 13 minutes, growth media was added to culture. Media was half-changed 3 to 4 days after initial culture.

Nocodazole Treatment

At 6 days in vitro (DIV), neurons were pretreated with DMSO or 500nM DLK inhibitor (GNE3511) resuspended in neurobasal (Gibco). After 15 minutes, neurons were then treated with DMSO, or 200nM nocodazole. This produced 4 groups ((1)DMSO, DMSO; (2) DMSO, Noc; (3) DLKi, DMSO and (4) DLKi, Noc). Neurons were collected for further analysis or imaging 16 hours after treatment.

Western Blot

Lysate buffers (60 mM Tri-HCl, pH 6.8; 50 % glycerol; 2 % SDS; 0.1 % bromophenol blue) contain protease cocktail (cOmplete, mini, EDTA-free protease inhibitor; 1183617001, Millipore Sigma) and phosphatase inhibitor cocktail (P0044, Millipore Sigma). Lysates were centrifuged at 4° for 5 minutes at 5,000g. Laemelli 6x Reducing buffer (Boston Biosciences) was added at 1x final concentration and boiled for 10 minutes. Samples were run on Mini-PROTEAN® TGX Precast Protein Gels (Bio-Rad Laboratories) and subsequently transferred to nitrocellulose membranes using Trans-Blot® Turbo Midi Nitrocellulose Transfer Packs (Bio-Rad Laboratories) on a Trans-Blot Turbo Transfer System. Membranes were blocked in TBS+0.1% tween and milk or 5% bovine serum albumin (Sigma-Aldrich, cat# A3912-50G) in TBS+0.1% tween (phospho- protein samples) for 60 minutes.

The following antibodies were used: 1:1000 rabbit anti-MKK4 (Cell Signaling Technologies 9152), 1:1000 rabbit anti-phospho-MKK4 (ser257/thr261) (Cell Signaling Technologies 9156),1:1000 rabbit anti-phosphorylated cJun (ser73) (Cell Signaling Technologies 3270S), 1:1000 rabbit anti-cJun (Cell Signaling Technologies 9165P), 1:1000 rabbit anti-HSP90 (Cell Signaling Technologies 4877S). Goat Anti-Rabbit IgG (Jackson ImmunoResearch Laboratories 111–035-045) . For phospho-proteins, membranes were stripped with Pierce™ Restore™ PLUS Western Blot Stripping Buffer(Thermo Scientific 46430) for 15 minutes at 37°, washed 3x 15 minutes and re-processed for non phosphorylated protein.

Sequencing

After nocodazole treatment, RNA was extracted from eDRGS. For each sample, 3 wells of a 12 well plate (corning) were polled. RNA extraction was performed using ReliaPrep RNA Cell Miniprep System (Promega). All biological replicates were performed on the same day. For each condition, 4 replicates were obtained.

Data Processing

Reads were processed using the nf-core/rnaseq workflow version 3.6 using STAR and Salmon for alignment and quantification and default settings. QC metrics from the nf-core pipeline, collected by multiqc, were inspected visually for evidence of outliers (see supplement). None were found. Differential expression analysis was performed using DESeq2 version 1.34.0 with an experiment design of ~researcher + pretreatment * treatment. The ashr method of shrinkage was applied to the coefficients (Stephens, 2017). The code used to execute DESeq2, extract the results, and perform the paper analysis is available at (https://github.com/Chase-Mateusiak/DLK_rnaseq).

qPCR

Biological replicates were obtained on independent days. RNA was collected and used to create cDNA library (Qscript, cDNA Supermix, Quanta bio). For each reaction, 80 ng cDNA was used. Each biological experiment was performed in triplicate. Obvious outliers in technical replicates were eliminated from further analysis. Technical replicates were averaged to create a biological replicate. Biological replicates with greater than 0.5 SD

were eliminated from further analysis. Pfaff method was used for quantification. Primer efficiency was calculated using pooled cDNA and 4x, 10 fold dilution series in an independent experiment.

Target	interest	efficiency	Forward Primer	Reverse Primer
ubc	housekeeping	97	GCCCAGTGTTACCACCAAGA	CCCATCACACCCAAGAACA
rpl27	housekeeping	108	AAGCCGTCATCGTGAAGAACA	CTTGATCTTGGATCGCTTGGC
zyx	actin	112.7	AGCGAGCCTCCTGTAGC	GGGCAAAGGAAAGTCTTCCG
itga9	actin	100	TCAAGTGCAGTGTGGGATTT	CAGTCACGATGAAGCTGAGAA
stmn4	cyto	90	GAACAGCTCGCTTTGGAAAC	CTGGAATCTGGTGGCTGAAT

GO Enrichment
In the DLKi in Noc data set, we ranked genes by log2FoldChange and selected the 500 greatest absolute value changes. This set was analyzed using gene set enrichment analysis with WebGestalt. Additional GO enrichment analysis was performed using gProfiler, using differentially expressed genes with a greater than absolute value log2foldchange greater than 0.5.

Immunhistochemistry
Neurons were cultured on 4 well slides. At 1DIV, neurons were transduced with GFP lentivirus. On 6DIV, neurons were treated with nocodazole and fixed for 10 minutes in 2%PFA. Samples were washed 3x 5 minutes and subsequently stained with Phalloidin, CF568 Conjugate (Biotium) for 30 minutes. Neurons were washed 2x 5 minutes and mounted using VECTASHIELD® HardSet™ Antifade Mounting Medium, Liquid (Vector Laboratories).

Quantification of neuronal morphology
To mark neuronal morphology, eDRGs were transduced with GFP lentivirus. FUGW (Addgene 14883)(200ng), vesicular stomatitis virus G (200 ng) and pSPAX2 (600 ng) using FuGENE 6 (Promega) were cotransfected into HEK 293 cells for lentivirus production HEK 293 cells were plated at 60% density the previous day. Lentiviral supernatant was collected after 2 days and applied to eDRG cultured at no greater than 10% volume.

Cell bodies were plated on the edge of 24 well plates (corning), to encourage axon and growth cone density in the center of the plate. At 6DIV, neurons were treated as described above. After 16 hours, neurons were imaged using the 40x lens of the IN Cell Analyzer 6000 (GE). For each well, 60 images were acquired and manual sorted for images with axon tips. These images were cropped to 150 x 150 pixel images. Images were subsequently processed in ImageJ using the following steps 1) Make 8bit. 2) Adjust Local Autocontrast (Phansalkar. Radius 15) 3) Invert image 4) Despeckle 5) Analyze Particles (Total Area, %Area, Particle Size: 5-infinity).

To stain for actin processes, neurons were cultured as described above. Neurons were fixed in 2% PFA for 10 minutes, and washed in PBST 3 x 5 minutes. Neurons were stained with Phalloidin, CF568 Conjugate (Biotium) for 30 minutes.

To quantify microtubule integrity, neurons were fixed in 2%PFA for 10 minutes, stained with Tuj1 (Rb, 1:1000; MAB1637, Sigma).Neurons were imaged at 20x on the IN Cell Analyzer 6000 (GE). Images were analyzed using the following steps 1) Make 8bit 2) Adjust Local Autocontrast (Phansalkar. Radius 25) 3) Analyze Particles (size

5-∞; circularity 0.5-1) 4) Collect %Area. Measurements were normalized to DMSO controls collected on the same day.

1.An N, Bassil K, Al Jowf GI, Steinbusch HWM, Rothermel M, de Nijs L, et al. Dual-specificity phosphatases in mental and neurological disorders. Progress in Neurobiology. 2021 Mar 1;198:101906.

2.Asghari Adib E, Smithson LJ, Collins CA. An axonal stress response pathway: degenerative and regenerative signaling by DLK. Current Opinion in Neurobiology. 2018 Dec 1;53:110–9.

3.Bossy-Wetzel E, Bakiri L, Yaniv M. Induction of apoptosis by the transcription factor c-Jun. The EMBO Journal. 1997 Apr;16(7):1695–709.

4.Cavalli V, Kujala P, Klumperman J, Goldstein LSB. Sunday Driver links axonal transport to damage signaling. J Cell Biol. 2005 Feb 28;168(5):775–87.

5.Chen L, Chuang M, Koorman T, Boxem M, Jin Y, Chisholm AD. Axon injury triggers EFA-6 mediated destabilization of axonal microtubules via TACC and doublecortin like kinase. VijayRaghavan K, editor. eLife. 2015 Sep 4;4:e08695.

6.Chuang M, Goncharov A, Wang S, Oegema K, Jin Y, Chisholm AD. The microtubule minus-end-binding protein patronin/PTRN-1 is required for axon regeneration in C. elegans. Cell Rep. 2014 Nov 6;9(3):874–83.

7.Collins CA, Wairkar YP, Johnson SL, DiAntonio A. Highwire restrains synaptic growth by attenuating a MAP kinase signal. Neuron. 2006 Jul 6;51(1):57–69.

8.Costa AR, Sousa SC, Pinto-Costa R, Mateus JC, Lopes CD, Costa AC, et al. The membrane periodic skeleton is an actomyosin network that regulates axonal diameter and conduction. Lappalainen P, Boudker O, Lappalainen P, Hotulainen P, Burnette DT, editors. eLife. 2020 Mar 20;9:e55471.

9.Dent EW, Kalil K. Axon Branching Requires Interactions between Dynamic Microtubules and Actin Filaments. J Neurosci. 2001 Dec 15;21(24):9757–69.

10.Dragunow M, Young D, Hughes P, MacGibbon G, Lawlor P, Singleton K, et al. Is c-Jun involved in nerve cell death following status epilepticus and hypoxic-ischaemic brain injury? Molecular Brain Research. 1993 Jun;18(4):347–52.

11.Ertürk A, Hellal F, Enes J, Bradke F. Disorganized Microtubules Underlie the Formation of Retraction Bulbs and the Failure of Axonal Regeneration. J Neurosci. 2007 Aug 22;27(34):9169–80.

12.Fan G, Merritt SE, Kortenjann M, Shaw PE, Holzman LB. Dual leucine zipper-bearing kinase (DLK) activates p46SAPK and p38mapk but not ERK2. J Biol Chem. 1996 Oct 4;271(40):24788–93.

13.Feng C, Thyagarajan P, Shorey M, Seebold DY, Weiner AT, Albertson RM, et al. Patronin-mediated minus end growth is required for dendritic microtubule polarity. J Cell Biol. 2019 Jul 1;218(7):2309–28.

14.Frey E, Valakh V, Karney-Grobe S, Shi Y, Milbrandt J, DiAntonio A. An in vitro assay to study induction of the regenerative state in sensory neurons. Exp Neurol. 2015 Jan;263:350–63.

15.Gallo G, Letourneau PC. Different Contributions of Microtubule Dynamics and Transport to the Growth of Axons and Collateral Sprouts. J Neurosci. 1999 May 15;19(10):3860–73.

16.Gazzola M, Schaeffer A, Butler-Hallissey C, Friedl K, Vianay B, Gaillard J, et al. Microtubules self-repair in living cells. Current Biology. 2023 Jan 9;33(1):122-133.e4.

17.Ghosh-Roy A, Goncharov A, Jin Y, Chisholm AD. Kinesin-13 and tubulin posttranslational modifications regulate microtubule growth in axon regeneration. Dev Cell. 2012 Oct 16;23(4):716–28.

18.Hammarlund M, Nix P, Hauth L, Jorgensen EM, Bastiani M. Axon regeneration requires a conserved MAP kinase pathway. Science. 2009 Feb 6;323(5915):802–6.

19..Harding HP, Zhang Y, Ron D. Protein translation and folding are coupled by an endoplasmic-reticulum-resident kinase. Nature. 1999 Jan;397(6716):271–4.

20.Hofmann M, Biller L, Michel U, Bähr M, Koch JC. Cytoskeletal assembly in axonal outgrowth and regeneration analyzed on the nanoscale. Sci Rep. 2022 Aug 23;12(1):14387.

21.Holland SM, Collura KM, Ketschek A, Noma K, Ferguson TA, Jin Y, et al. Palmitoylation controls DLK localization, interactions and activity to ensure effective axonal injury signaling. Proceedings of the National Academy of Sciences. 2016 Jan 19;113(3):763–8.

22.Huntwork-Rodriguez S, Wang B, Watkins T, Ghosh AS, Pozniak CD, Bustos D, et al. JNK-mediated phosphorylation of DLK suppresses its ubiquitination to promote neuronal apoptosis. J Cell Biol. 2013 Sep 2;202(5):747–63.

23..Itoh T, Horiuchi M, Ikeda RH, Xu J, Bannerman P, Pleasure D, et al. ZPK/DLK and MKK4 Form the Critical Gateway to Axotomy-Induced Motoneuron Death in Neonates. J Neurosci. 2014 Aug 6;34(32):10729–42.

24.Jacobi A, Tran NM, Yan W, Benhar I, Tian F, Schaffer R, et al. Overlapping transcriptional programs promote survival and axonal regeneration of injured retinal ganglion cells. Neuron. 2022 Aug 17;110(16):2625-2645.e7.

25.Jaworski J, Kapitein LC, Gouveia SM, Dortland BR, Wulf PS, Grigoriev I, et al. Dynamic Microtubules Regulate Dendritic Spine Morphology and Synaptic Plasticity. Neuron. 2009 Jan 15;61(1):85–100.

26.Jeanneteau F, Deinhardt K, Miyoshi G, Bennett AM, Chao MV. The MAP kinase phosphatase MKP-1 regulates BDNF-induced axon branching. Nat Neurosci. 2010 Nov;13(11):1373–9.

27.Karney-Grobe S, Russo A, Frey E, Milbrandt J, DiAntonio A. HSP90 is a chaperone for DLK and is required for axon injury signaling. Proceedings of the National Academy of Sciences. 2018 Oct 16;115(42):E9899–908.

28.Kerschensteiner M, Schwab ME, Lichtman JW, Misgeld T. In vivo imaging of axonal degeneration and regeneration in the injured spinal cord. Nat Med. 2005 May;11(5):572–7.

29. Kleele T, Marinković P, Williams PR, Stern S, Weigand EE, Engerer P, et al. An assay to image neuronal microtubule dynamics in mice. Nat Commun. 2014 Sep 12;5(1):4827.

30.Larhammar M, Huntwork-Rodriguez S, Jiang Z, Solanoy H, Sengupta Ghosh A, Wang B, et al. Dual leucine zipper kinase-dependent PERK activation contributes to neuronal degeneration following insult. Dillin A, editor. eLife. 2017 Apr 25;6:e20725.

31.Leterrier C. Putting the axonal periodic scaffold in order. Current Opinion in Neurobiology. 2021 Aug 1;69:33–40.

32.Lindwall C, Dahlin L, Lundborg G, Kanje M. Inhibition of c-Jun phosphorylation reduces axonal outgrowth of adult rat nodose ganglia and dorsal root ganglia sensory neurons. Molecular and Cellular Neuroscience. 2004 Nov 1;27(3):267–79.

33.Liu Y, DeBoer K, de Kretser DM, O'Donnell L, O'Connor AE, Merriner DJ, et al. LRGUK-1 Is Required for Basal Body and Manchette Function during Spermatogenesis and Male Fertility. PLoS Genet. 2015 Mar 17;11(3):e1005090.

34. Lu W, Lakonishok M, Gelfand VI. Kinesin-1-powered microtubule sliding initiates axonal regeneration in Drosophila cultured neurons. Mol Biol Cell. 2015 Apr 1;26(7):1296–307.

35.Maor-Nof M, Romi E, Sar Shalom H, Ulisse V, Raanan C, Nof A, et al. Axonal Degeneration Is Regulated by a Transcriptional Program that Coordinates Expression of Pro- and Anti-degenerative Factors. Neuron. 2016 Dec 7;92(5):991–1006.

36.Mattila PK, Lappalainen P. Filopodia: molecular architecture and cellular functions. Nat Rev Mol Cell Biol. 2008 Jun;9(6):446–54.

37.Messaoudi E, Kanhema T, Soulé J, Tiron A, Dagyte G, da Silva B, et al. Sustained Arc/Arg3.1 synthesis controls long-term potentiation consolidation through regulation of local actin polymerization in the dentate gyrus in vivo. J Neurosci. 2007 Sep 26;27(39):10445–55.

38. Milbrandt,J. A nerve growth factor-induced gene encodes a possible transcriptional regulatory factor. Science (New York, NY) [Internet]. 1987 Nov 6 [cited 2023 Aug 22];238(4828). Available from: https://pubmed.ncbi.nlm.nih.gov/3672127/

39.Miller BR, Press C, Daniels RW, Sasaki Y, Milbrandt J, DiAntonio A. A dual leucine kinase-dependent axon self-destruction program promotes Wallerian degeneration. Nat Neurosci. 2009 Apr;12(4):387–9.

40.Nakao C, Itoh TJ, Hotani H, Mori N. Modulation of the stathmin-like microtubule destabilizing activity of RB3, a neuron-specific member of the SCG10 family, by its N-terminal domain. J Biol Chem. 2004 May 28;279(22):23014–21.

41.Nakata K, Abrams B, Grill B, Goncharov A, Huang X, Chisholm AD, et al. Regulation of a DLK-1 and p38 MAP kinase pathway by the ubiquitin ligase RPM-1 is required for presynaptic development. Cell. 2005 Feb 11;120(3):407–20.

42.Pakos-Zebrucka K, Koryga I, Mnich K, Ljujic M, Samali A, Gorman AM. The integrated stress response. EMBO Rep. 2016 Oct;17(10):1374–95.

43.Peck JW, Oberst M, Bouker KB, Bowden E, Burbelo PD. The RhoA-binding protein, Rhophilin-2, Regulates Actin Cytoskeleton Organization *. Journal of Biological Chemistry. 2002 Nov 15;277(46):43924–32.

44.Pongrakhananon V, Saito H, Hiver S, Abe T, Shioi G, Meng W, et al. CAMSAP3 maintains neuronal polarity through regulation of microtubule stability. Proc Natl Acad Sci U S A. 2018 Sep 25;115(39):9750–5.

45.Qu Y, Hahn I, Webb SED, Pearce SP, Prokop A. Periodic actin structures in neuronal axons are required to maintain microtubules. Mol Biol Cell. 2017 Jan 15;28(2):296–308.

46.Renthal W, Tochitsky I, Yang L, Cheng YC, Li E, Kawaguchi R, et al. Transcriptional reprogramming of distinct peripheral sensory neuron subtypes after axonal injury. Neuron. 2020 Oct 14;108(1):128-144.e9.

47.Richardson CE, Spilker KA, Cueva JG, Perrino J, Goodman MB, Shen K. PTRN-1, a microtubule minus end-binding CAMSAP homolog, promotes microtubule function in Caenorhabditis elegans neurons. Hobert O, editor. eLife. 2014 Feb 25;3:e01498.

48.Sengupta Ghosh A, Wang B, Pozniak CD, Chen M, Watts RJ, Lewcock JW. DLK induces developmental neuronal degeneration via selective regulation of proapoptotic JNK activity. Journal of Cell Biology. 2011 Sep 5;194(5):751–64.

49. Shi Y, Vattem KM, Sood R, An J, Liang J, Stramm L, et al. Identification and Characterization of Pancreatic Eukaryotic Initiation Factor 2 α-Subunit Kinase, PEK, Involved in Translational Control. Molecular and Cellular Biology. 1998 Dec 1;18(12):7499–509.

50.Shin JE, Cho Y, Beirowski B, Milbrandt J, Cavalli V, DiAntonio A. Dual leucine zipper kinase is required for retrograde injury signaling and axonal regeneration. Neuron. 2012 Jun 21;74(6):1015–22.

51.Shin JE, Ha H, Kim YK, Cho Y, DiAntonio A. DLK regulates a distinctive transcriptional regeneration program after peripheral nerve injury. Neurobiol Dis. 2019 Jul;127:178–92.

52.Silva RC, Sattlegger E, Castilho BA. Perturbations in actin dynamics reconfigure protein complexes that modulate GCN2 activity and promote an eIF2 response. Journal of Cell Science. 2016 Dec 15;129(24):4521–33.

53.Sood R, Porter AC, Ma K, Quillam, LA, Wek RC. Pancreatic eukaryotic initiation factor-2α kinase (PEK) homologues in humans, Drosophila melanogaster and Caenorhabditis elegans that mediate translational control in response to endoplasmic reticulum stress. Biochemical Journal. 2000 Feb 22;346(2):281–93.

54.Stephens M. False discovery rates: a new deal. Biostatistics. 2017 Apr 1;18(2):275–94.

55.Stern S, Hilton BJ, Burnside ER, Dupraz S, Handley EE, Gonyer JM, et al. RhoA drives actin compaction to restrict axon regeneration and astrocyte reactivity after CNS injury. Neuron. 2021 Nov 3;109(21):3436-3455.e9.

56.Taylor DM, Moser R, Régulier E, Breuillaud L, Dixon M, Beesen AA, et al. MAP Kinase Phosphatase 1 (MKP-1/DUSP1) Is Neuroprotective in Huntington's Disease via Additive Effects of JNK and p38 Inhibition. J Neurosci. 2013 Feb 6;33(6):2313–25.

57. Tedeschi A, Dupraz S, Curcio M, Laskowski CJ, Schaffran B, Flynn KC, et al. ADF/Cofilin-Mediated Actin Turnover Promotes Axon Regeneration in the Adult CNS. Neuron. 2019 Sep 25;103(6):1073-1085.e6.

58. Tian F, Cheng Y, Zhou S, Wang Q, Monavarfeshani A, Gao K, et al. Core Transcription Programs Controlling Injury-Induced Neurodegeneration of Retinal Ganglion Cells. Neuron. 2022 Aug 17;110(16):2607-2624.e8.

59. Tian R, Gachechiladze MA, Ludwig CH, Laurie MT, Hong JY, Nathaniel D, et al. CRISPR Interference-Based Platform for Multimodal Genetic Screens in Human iPSC-Derived Neurons. Neuron. 2019 Oct 23;104(2):239-255.e12.

60.Tian X, Li J, Valakh V, DiAntonio A, Wu C. Drosophila Rae1 controls the abundance of the ubiquitin ligase Highwire in post-mitotic neurons. Nat Neurosci. 2011 Aug 28;14(10):1267–75.

61.Tortosa E, Sengupta Ghosh A, Li Q, Wong WR, Hinkle T, Sandoval W, et al. Stress-induced vesicular assemblies of dual leucine zipper kinase are signaling hubs involved in kinase activation and neurodegeneration. The EMBO Journal. 2022 Jul 18;41(14):e110155.

62. Unsain N, Bordenave MD, Martinez GF, Jalil S, von Bilderling C, Barabas FM, et al. Remodeling of the Actin/Spectrin Membrane-associated Periodic Skeleton, Growth Cone Collapse and F-Actin Decrease during Axonal Degeneration. Sci Rep. 2018 Feb 14;8(1):3007.

63. Unsain N, Stefani FD, Cáceres A. The Actin/Spectrin Membrane-Associated Periodic Skeleton in Neurons. Front Synaptic Neurosci. 2018;10:10.

64. Valakh V, Frey E, Babetto E, Walker LJ, DiAntonio A. Cytoskeletal disruption activates the DLK/JNK pathway, which promotes axonal regeneration and mimics a preconditioning injury. Neurobiol Dis. 2015 May;77:13–25.

65. Valakh V, Walker LJ, Skeath JB, DiAntonio A. Loss of the spectraplakin short stop activates the DLK injury response pathway in Drosophila. J Neurosci. 2013 Nov 6;33(45):17863–73.

66. Wang G, Simon DJ, Wu Z, Belsky DM, Heller E, O'Rourke MK, et al. Structural plasticity of actin-spectrin membrane skeleton and functional role of actin and spectrin in axon degeneration. Elife. 2019 May 1;8:e38730.

67. Wang X, Kim JH, Bazzi M, Robinson S, Collins CA, Ye B. Bimodal control of dendritic and axonal growth by the dual leucine zipper kinase pathway. PLoS Biol. 2013;11(6):e1001572.

68. Watkins TA, Wang B, Huntwork-Rodriguez S, Yang J, Jiang Z, Eastham-Anderson J, et al. DLK initiates a transcriptional program that couples apoptotic and regenerative responses to axonal injury. Proc Natl Acad Sci U S A. 2013 Mar 5;110(10):4039–44.

69. Welsbie DS, Yang Z, Ge Y, Mitchell KL, Zhou X, Martin SE, et al. Functional genomic screening identifies dual leucine zipper kinase as a key mediator of retinal ganglion cell death. Proc Natl Acad Sci U S A. 2013 Mar 5;110(10):4045–50.

70. Xiong X, Wang X, Ewanek R, Bhat P, Diantonio A, Collins CA. Protein turnover of the Wallenda/DLK kinase regulates a retrograde response to axonal injury. J Cell Biol. 2010 Oct 4;191(1):211–23.

71. Xu K, Zhong G, Zhuang X. Actin, spectrin, and associated proteins form a periodic cytoskeletal structure in axons. Science. 2013 Jan 25;339(6118):452–6.

72. Yang J, Wu Z, Renier N, Simon DJ, Uryu K, Park DS, et al. Pathological Axonal Death through a MAPK Cascade that Triggers a Local Energy Deficit. Cell. 2015 Jan 15;160(1):161–76.

73. Yin F, Liu Z, Zhang D, Shen Z, Niu Z, Guo L. Identification of key genes involved in neural regeneration and the repairing effect of BDNF-overexpressed BMSCs on spinal cord ischemia-reperfusion injury in rats. Biomedicine & Pharmacotherapy. 2023 Apr 1;160:114293.

74. Zhang Y, Abiraman K, Li H, Pierce DM, Tzingounis AV, Lykotrafitis G. Modeling of the axon membrane skeleton structure and implications for its mechanical properties. PLOS Computational Biology. 2017 Feb 27;13(2):e1005407.

75. Zhong G, He J, Zhou R, Lorenzo D, Babcock HP, Bennett V, et al. Developmental mechanism of the periodic membrane skeleton in axons. Singer RH, editor. eLife. 2014 Dec 23;3:e04581.

Fig. 1

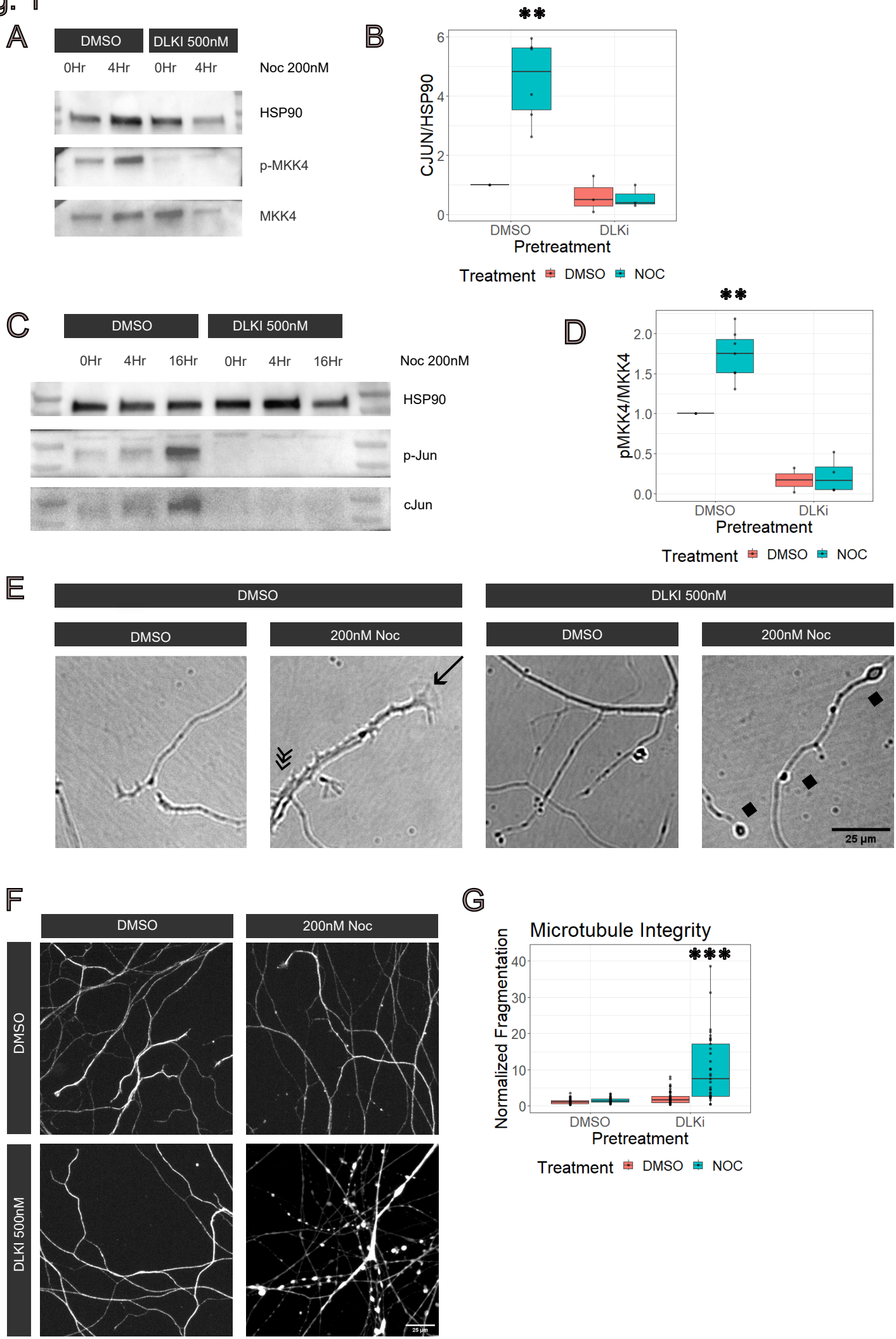
A
DMSO
DLKI 500nM
0Hr
4Hr
0Hr
4Hr
Noc 200nM
HSP90
p-MKK4
MKK4
B
**
CJUN/HSP90
6
4
2
0
DMSO
DLKi
Pretreatment
Treatment
DMSO
NOC
C
DMSO
DLKI 500nM
0Hr
4Hr
16Hr
0Hr
4Hr
16Hr
Noc 200nM
HSP90
p-Jun
cJun
D
**
pMKK4/MKK4
2.0
1.5
1.0
0.5
0.0
DMSO
DLKi
Pretreatment
Treatment
DMSO
NOC
E
DMSO
DLKI 500nM
DMSO
200nM Noc
DMSO
200nM Noc
25 µm
F
DMSO
200nM Noc
DMSO
DLKI 500nM
G
Microtubule Integrity
***
Normalized Fragmentation
40
30
20
10
0
DMSO
DLKi
Pretreatment
Treatment
DMSO
NOC

Fig. 2

A

Pretreatment
Treatment
DMSO, DMSO
DLKi, DMSO
DMSO, Noc
DLKi, Noc

B

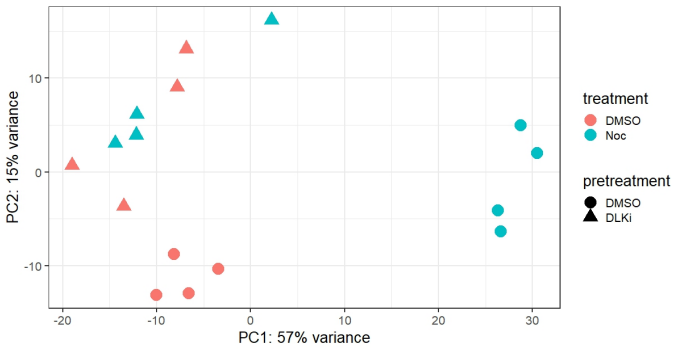
PC2: 15% variance
PC1: 57% variance
treatment
DMSO
Noc
pretreatment
DMSO
DLKi

C

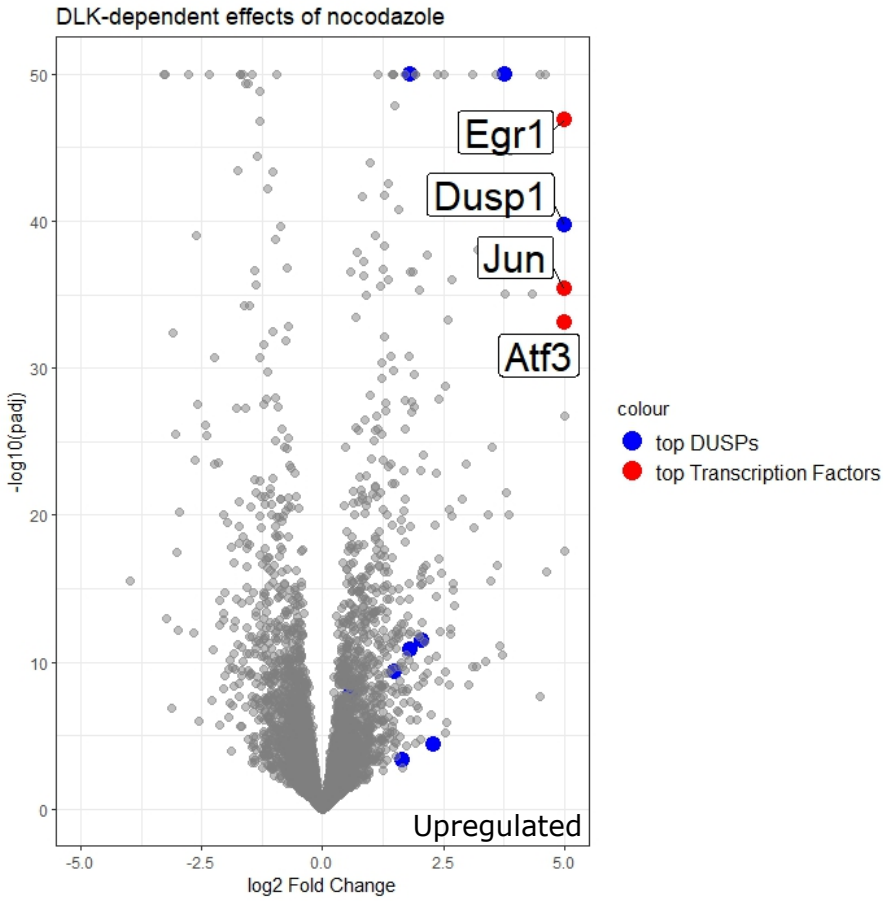
DLK-dependent effects of nocodazole
Egr1
Dusp1
Jun
Atf3
Upregulated
-log10(padj)
log2 Fold Change
colour
top DUSPs
top Transcription Factors

D

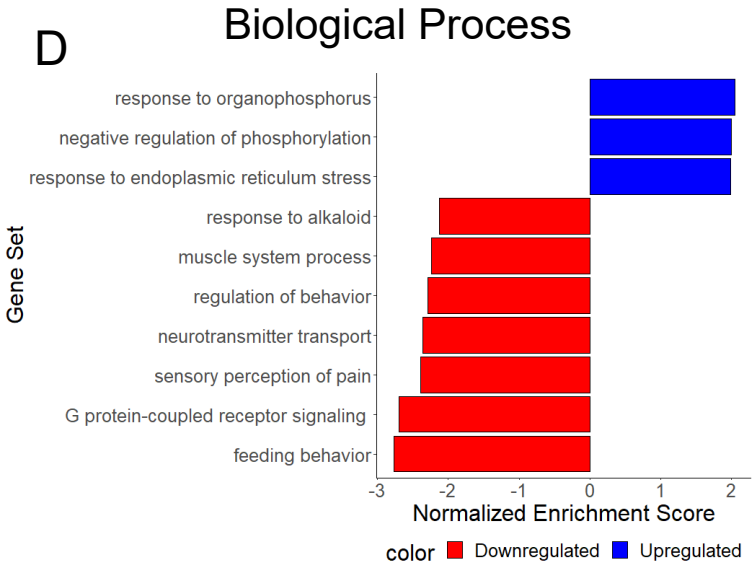
Biological Process
response to organophosphorus
negative regulation of phosphorylation
response to endoplasmic reticulum stress
response to alkaloid
muscle system process
regulation of behavior
neurotransmitter transport
sensory perception of pain
G protein-coupled receptor signaling
feeding behavior
Gene Set
Normalized Enrichment Score
color
Downregulated
Upregulated

E

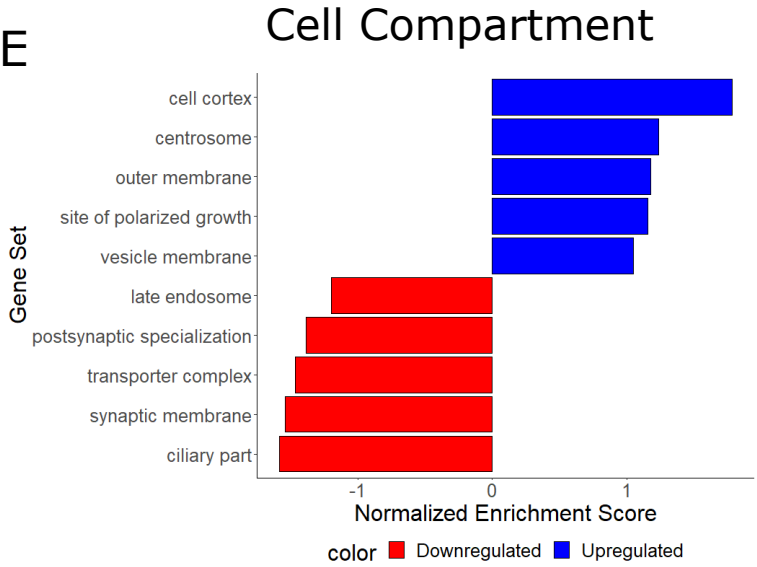
Cell Compartment
cell cortex
centrosome
outer membrane
site of polarized growth
vesicle membrane
late endosome
postsynaptic specialization
transporter complex
synaptic membrane
ciliary part
Gene Set
Normalized Enrichment Score
color
Downregulated
Upregulated

F

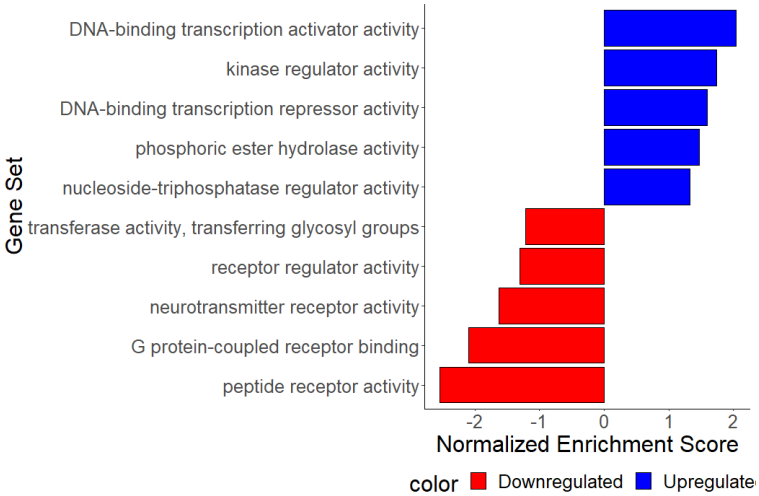
Molecular Function
DNA-binding transcription activator activity
kinase regulator activity
DNA-binding transcription repressor activity
phosphoric ester hydrolase activity
nucleoside-triphosphatase regulator activity
transferase activity, transferring glycosyl groups
receptor regulator activity
neurotransmitter receptor activity
G protein-coupled receptor binding
peptide receptor activity
Gene Set
Normalized Enrichment Score
color
Downregulated
Upregulate

Fig. 3

A

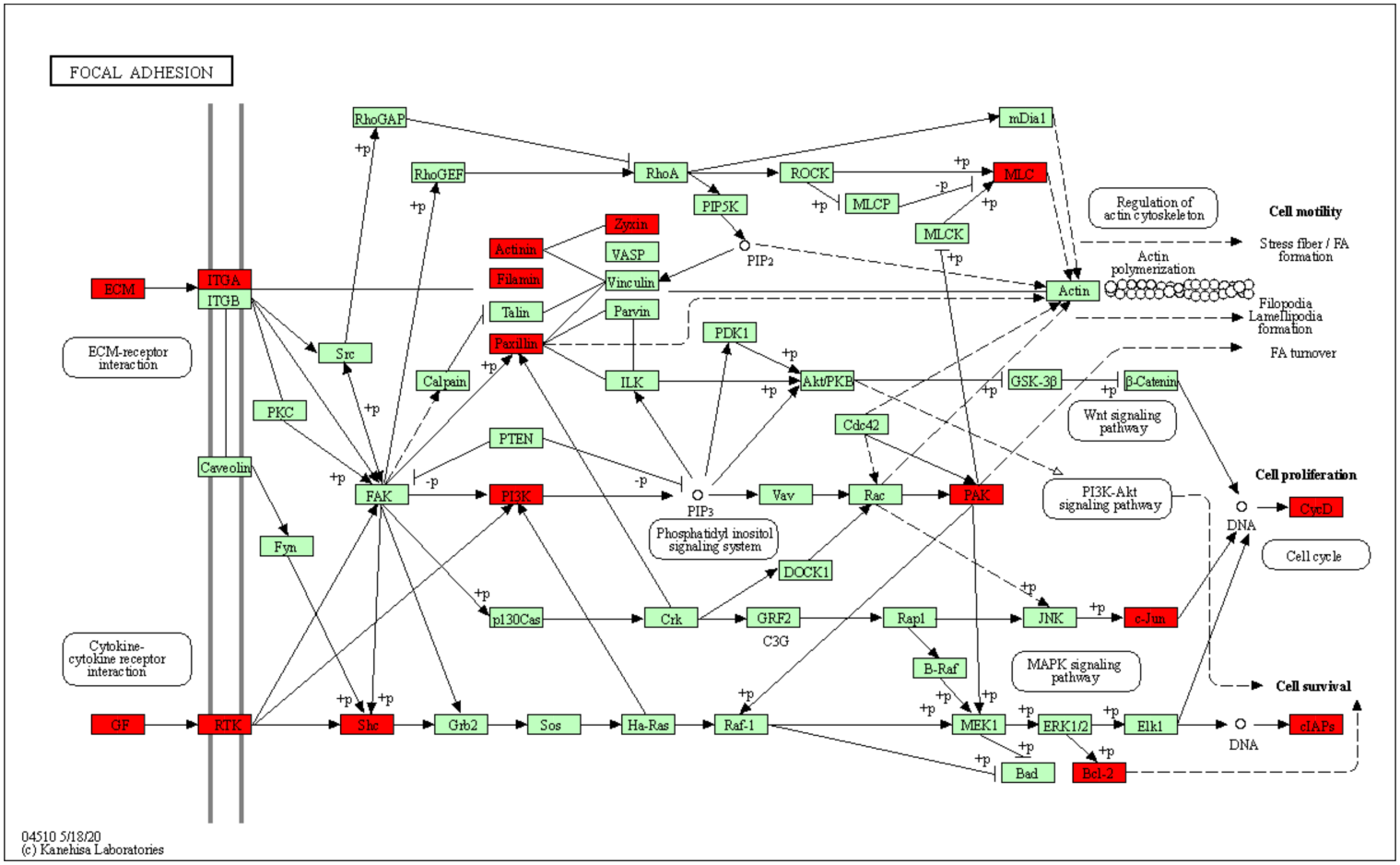
FOCAL ADHESION
ECM
ITGA
ITGB
ECM-receptor interaction
RhoGAP
RhoGEF
RhoA
ROCK
mDia1
MLC
MLCP
MLCK
PIP5K
PIP2
Zyxin
VASP
Vinculin
Parvin
Actinin
Filamin
Talin
Paxillin
Actin
Regulation of actin cytoskeleton
Cell motility
Stress fiber / FA formation
Actin polymerization
Filopodia
Lamellipodia formation
FA turnover
Src
Calpain
PKC
Caveolin
Fyn
FAK
PTEN
PI3K
ILK
PDK1
Akt/PKB
GSK-3β
β-Catenin
Wnt signaling pathway
Cdc42
Rac
PAK
PIP3
Phosphatidyl inositol signaling system
Vav
PI3K-Akt signaling pathway
Cell proliferation
CycD
DNA
Cell cycle
DOCK1
p130Cas
Crk
GRF2
C3G
Rap1
JNK
c-Jun
B-Raf
MAPK signaling pathway
Cell survival
Cytokine-cytokine receptor interaction
GF
RTK
Shc
Grb2
Sos
Ha-Ras
Raf-1
MEK1
ERK1/2
Elk1
cIAPs
Bad
Bcl-2
04510 5/18/20
(c) Kanehisa Laboratories

B

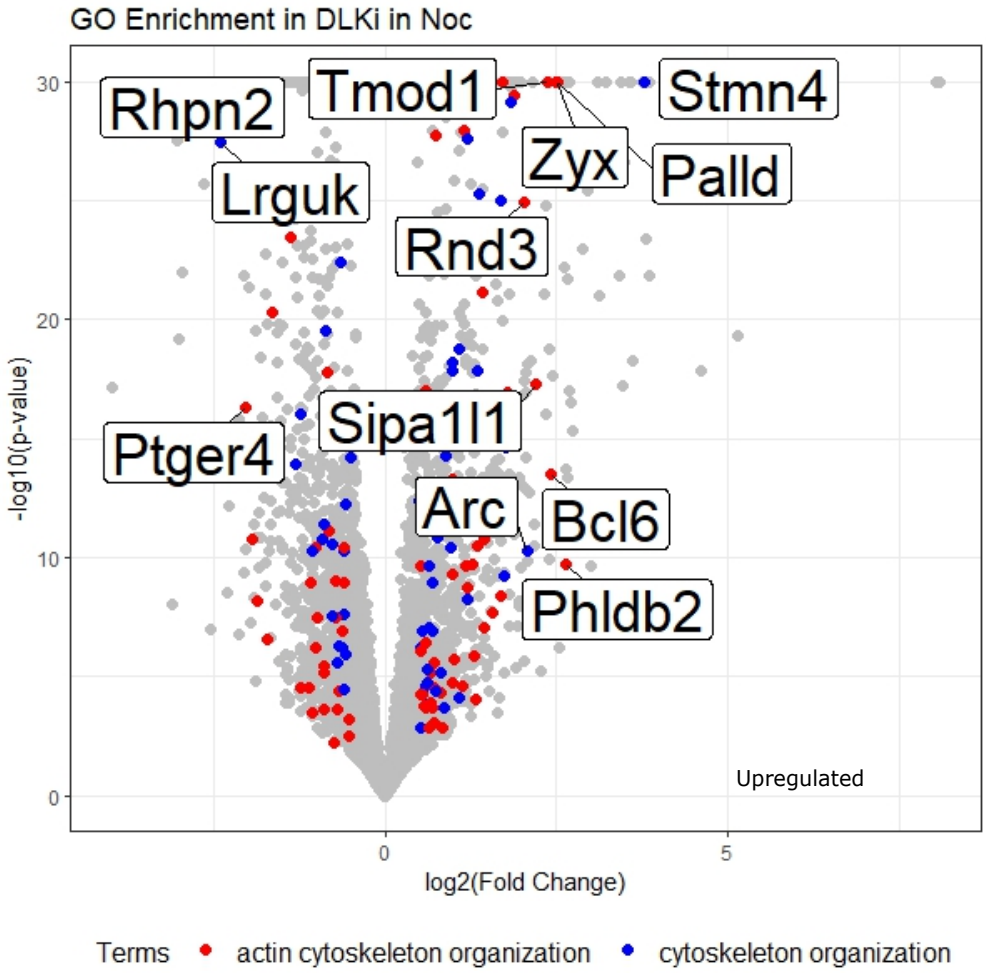
GO Enrichment in DLKi in Noc
Rhpn2
Tmod1
Stmn4
Zyx
Palld
Lrguk
Rnd3
Sipa1l1
Ptger4
Arc
Bcl6
Phldb2
Upregulated
-log10(p-value)
log2(Fold Change)
Terms
actin cytoskeleton organization
cytoskeleton organization

C

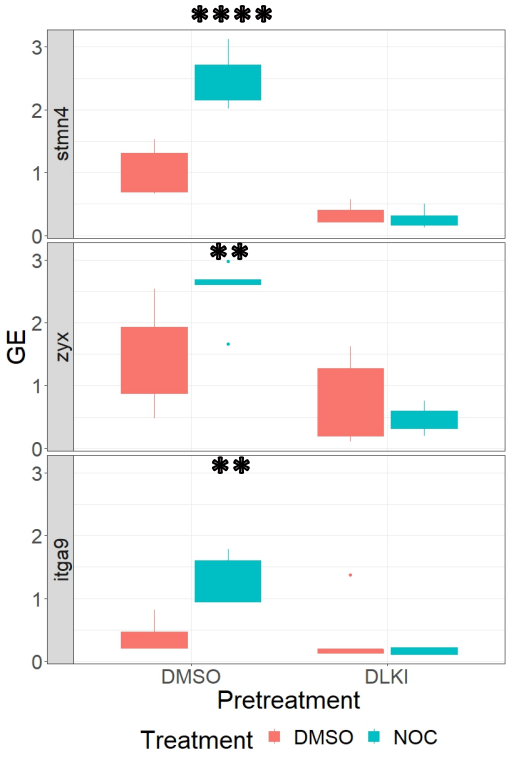
****
**
**
stmn4
zyx
itga9
GE
DMSO
DLKI
Pretreatment
Treatment
DMSO
NOC

Fig. 4

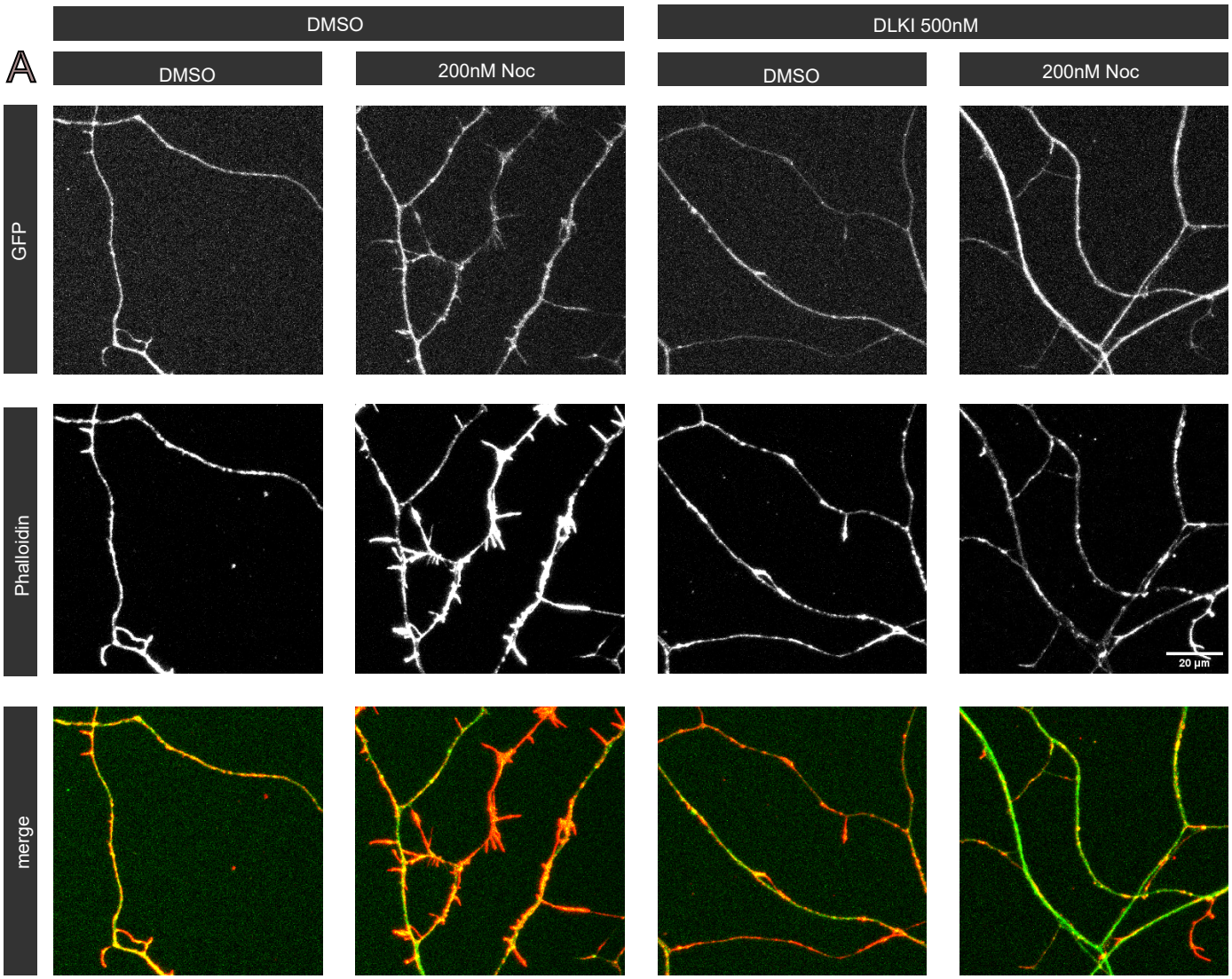
A
DMSO
DLKI 500nM
DMSO
200nM Noc
DMSO
200nM Noc
GFP
Phalloidin
merge
20 µm

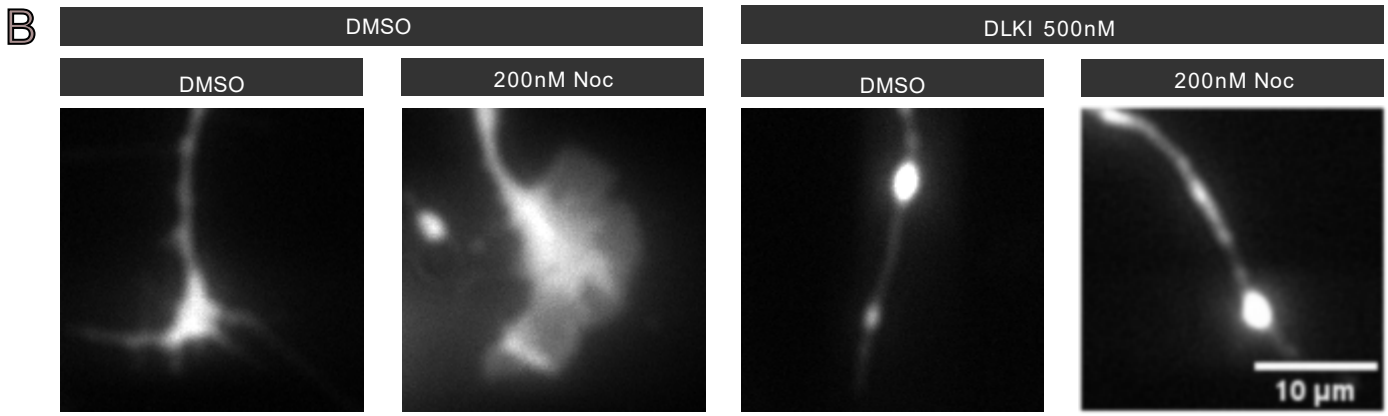
B
DMSO
DLKI 500nM
DMSO
200nM Noc
DMSO
200nM Noc
10 µm

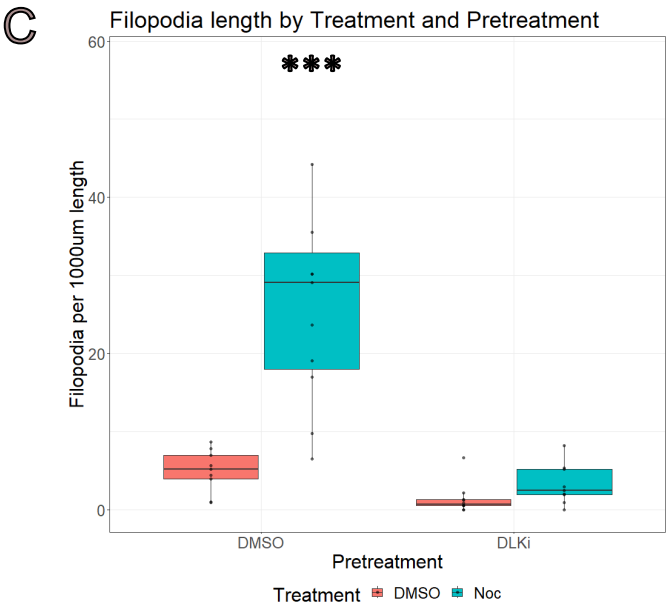
C
Filopodia length by Treatment and Pretreatment
***
Filopodia per 1000um length
0
20
40
60
DMSO
DLKi
Pretreatment
Treatment
DMSO
Noc

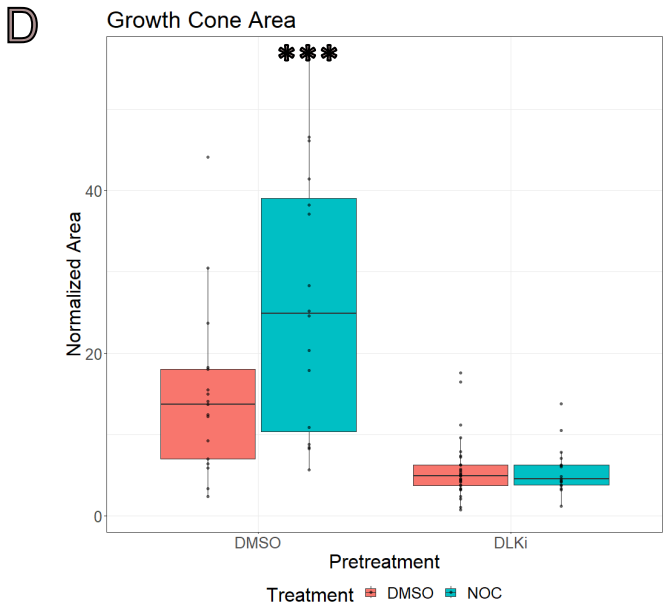
D
Growth Cone Area
***
Normalized Area
0
20
40
DMSO
DLKi
Pretreatment
Treatment
DMSO
NOC

Fig. 5

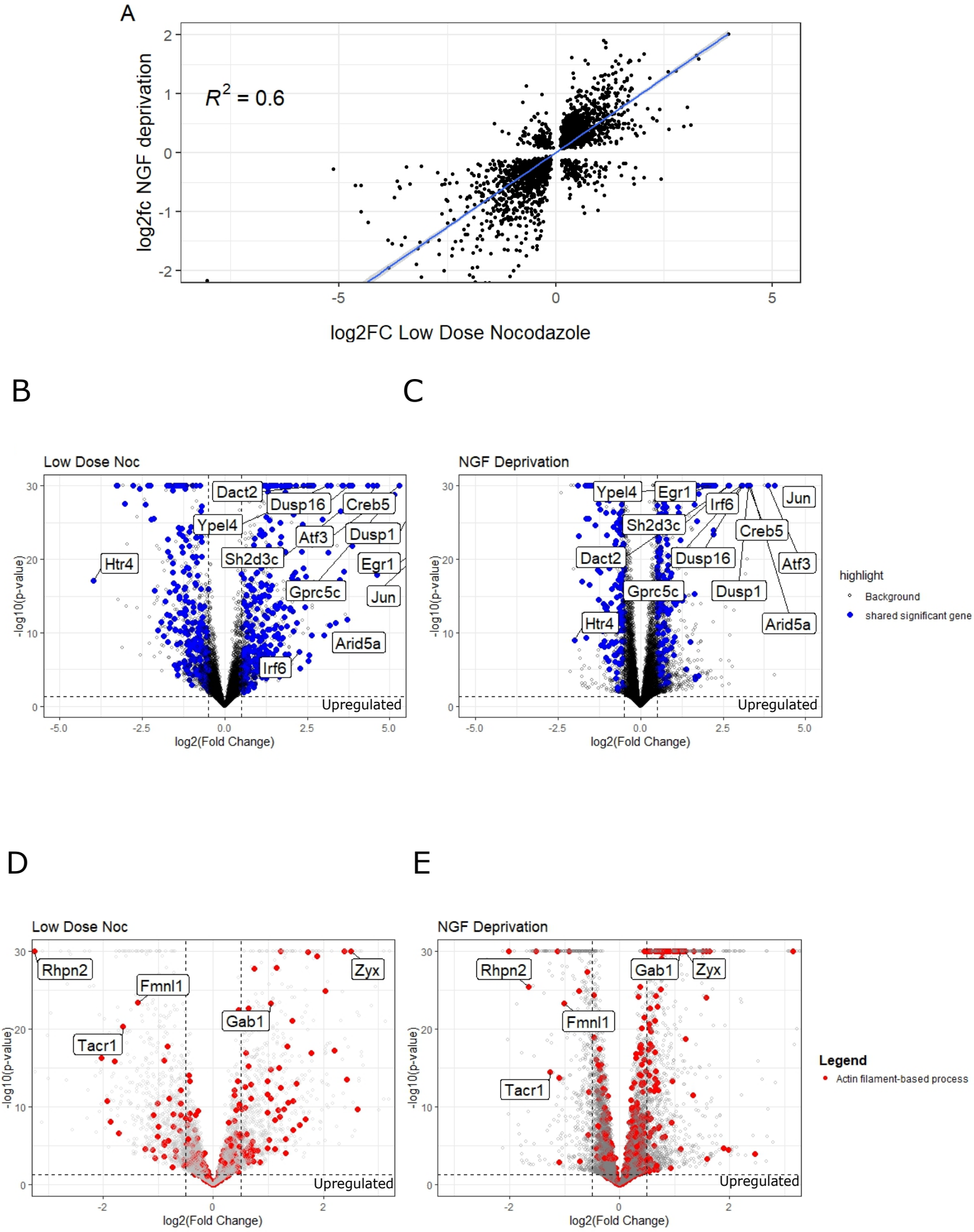
A
R^2 = 0.6
log2fc NGF deprivation
log2FC Low Dose Nocodazole
B
Low Dose Noc
Dact2
Dusp16
Creb5
Ypel4
Atf3
Dusp1
Htr4
Sh2d3c
Egr1
Gprc5c
Jun
Arid5a
Irf6
Upregulated
-log10(p-value)
log2(Fold Change)
C
NGF Deprivation
Ypel4
Egr1
Irf6
Jun
Sh2d3c
Creb5
Dact2
Dusp16
Atf3
Gprc5c
Dusp1
Htr4
Arid5a
Upregulated
-log10(p-value)
log2(Fold Change)
highlight
Background
shared significant gene
D
Low Dose Noc
Rhpn2
Fmnl1
Zyx
Gab1
Tacr1
Upregulated
-log10(p-value)
log2(Fold Change)
E
NGF Deprivation
Rhpn2
Gab1
Zyx
Fmnl1
Tacr1
Upregulated
-log10(p-value)
log2(Fold Change)
Legend
Actin filament-based process